§23. High Energy Ion Tail Production in ICRF Heating

Mutoh, T.

In the optimum conditions of ICRF heating in the 3rd campaign, the main wave damping mechanism was ion cyclotron damping by minority ions. It is so-called minority-heating mode. On the minority-heating mode, the high-energy ion tail was usually produced in many tokamaks and helical devices. In heliotron devices, the high-energy ions accelerated by ICRF were used to examine the confinement performance of the devices. In Heliotron E, ATF and CHS, the high-energy ion tails were observed and its confinement properties were examined. Those devices have small minor radiuses less than 20 cm, therefore the confinement properties were not sufficient. The high-energy particles were directly lost from the confinement region and caused impurity problems.

In LHD, the confinement of the high-energy ions is also one of the major concerns of the experiment. The high-energy ions produced by ICRF were observed on the neutral particle detectors. High-energy protons up to 300 keV were detected by natural diamond NPA detectors. In Fig.1, the tail temperatures, Ti_tail, defined by the energy range of 30-110 keV are shown with electron temperature, density and ICRF and NBI powers. In case of Fig. 1(a),

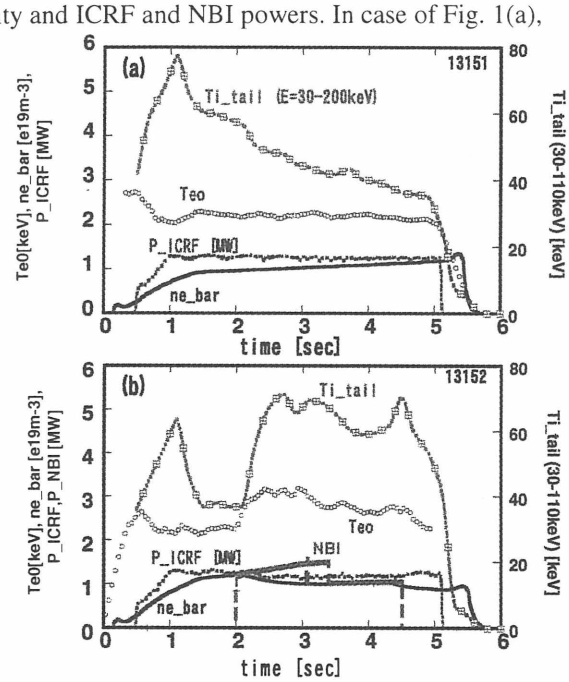

Fig.1 Temporal behavior of the tail temperature, Te and n_e with ICRF and NBI heating powers.

Ti_tail were decreased from 80 keV to 40 keV as density gradually increasing. To check the other parameter dependences on tail temperature, an NBI was applied additionally to ICRF sustained plasma as shown in Fig. 1(b). The NBI pulse was added from 2 to 4.5 sec and electron temperature of central region was raised from 2.2keV to around 3 keV. The tail temperature, Ti_tail, were raised from 40 to 70 keV as shown in the figure. In this case, electron temperature was effective to change the tail temperature.

The velocity-space distribution function for the minority ion can be estimated theoretically from Stix's formula. In the high-energy region, the tail temperature, Ti_tail, approaches the asymptotic value, T_{eff}.

$$T_{eff} \cong T_e(1+\xi) = T_e \times \left(1 + \frac{\langle P_\perp \rangle t_s}{3nT_e}\right)$$

where ξ is a dimensionless parameter directly proportional to the input power density, $\langle P_\perp \rangle$, and t_s is a Spitzer's slowing down time. Finally, T_{eff} is proportional to $\langle P_\perp \rangle T_e^{1.5}/n \cdot n_e$. Here n is the minority ion density. This effective tail temperature is the solution for the steady-state balance between the heating acceleration and the electron relaxation. In Fig. 2, the experimentally obtained Ti_tail in the two discharges are plotted against a parameter that is proportional to the T_{eff}. Here n, $\langle P_\perp \rangle$ and Te in the above equation are assumed to be proportional to the line-averaged density, input ICRF power, and central electron temperature, respectively. The data of the two discharges are in quite good agreement with the solid line, which indicates that the tail temperature is consistent with the Stix's formula.

This agreement supports the proposition that the wave-induced proton distribution is entirely balanced by the electron drag on the two discharges. High-energy particles with energies up to 300 keV were observed in the higher range of the horizontal-axis, where the input power is large, the electron temperature is high and the accelerated-particle density is small. The tail temperature does not show any saturation tendency in Fig.2, suggesting that ICRF power produces no particle orbit-loss effects for highly accelerated ions in the perpendicular direction. The stored energy of the plasma was proportional to the input ICRF power in the density range of over 1×10^{19} m^{-3}. These data also supported the premise that the particle-loss effect was negligibly small.

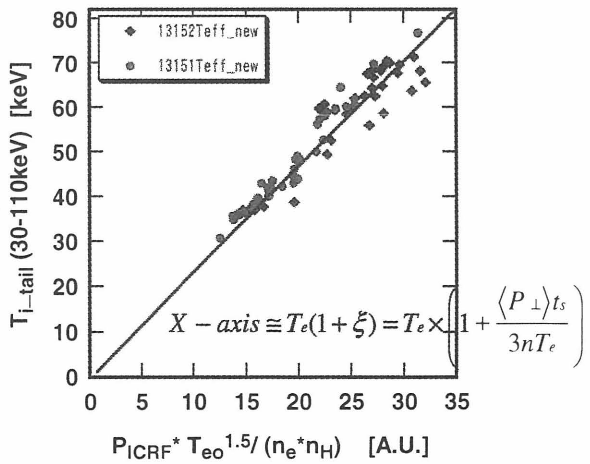

Fig.2 Tail temperatures of the Fig.1 are plotted against a parameter proportional to the Stix's effective tail temperatures.

Reference:

1) T. Mutoh, R. Kumazawa, et al., Plasma Physics and Controlled Fusion, 42, (2000) pp265-274